HHS Public Access

Author manuscript

J Immunol. Author manuscript; available in PMC 2016 July 01.

Published in final edited form as:

J Immunol. 2015 July 1; 195(1): 61–70. doi:10.4049/jimmunol.1400803.

Bruton's Tyrosine Kinase Synergizes with Notch2 to Govern Marginal Zone B Cells in Nonobese Diabetic Mice[1,,2]

James B. Case[#*,†], **Rachel H. Bonami**[#*], **Lindsay E. Nyhoff**[†], **Hannah E. Steinberg**[*], **Allison M. Sullivan**[*], and **Peggy L. Kendall**[*,†]

[*] Department of Medicine, Vanderbilt University Medical Center, Nashville, TN

[†] Department of Pathology, Microbiology and Immunology, Vanderbilt University Medical Center, Nashville, TN

[#] These authors contributed equally to this work.

Abstract

Expansion of autoimmune-prone marginal zone (MZ) B cells has been implicated in type 1 diabetes (T1D). To test disease contributions of MZ B cells in NOD mice, Notch2 haploinsufficiency (*Notch2*$^{+/-}$) was introduced, but failed to eliminate the MZ, as it does in C57BL/6 mice. *Notch2*$^{+/-}$*/NOD* have MZ B cell numbers similar to WT C57BL/6, yet still develop diabetes. To test whether BCR-signaling supports *Notch2*$^{+/-}$/NOD MZ B cells, Bruton's tyrosine kinase (*Btk*)-deficiency was introduced. Surprisingly, MZ B cells failed to develop in *Btk*-deficient *Notch2*$^{+/-}$/NOD mice. Expression of *Notch2* and its transcriptional target, *Hes5*, were increased in NOD MZ B cells compared with C57BL/6 MZ B cells. *Btk*-deficiency reduced *Notch2*$^{+/-}$ signaling exclusively in NOD B cells, suggesting that BCR-signaling enhances Notch2 signaling in this autoimmune model. The role of BCR-signaling was further investigated using an anti-insulin transgenic BCR (125Tg). Anti-insulin B cells in 125Tg/*Notch2*$^{+/-}$/NOD mice populate an enlarged MZ, suggesting that low level BCR signaling overcomes reliance on Notch2. Tracking clonotypes of anti-insulin B cells in H chain only V_H125Tg/NOD mice showed that BTK-dependent selection into the MZ depends on strength of antigenic binding, while Notch2-mediated selection does not. Importantly, anti-insulin B cell numbers were reduced by *Btk*-deficiency, but not *Notch2*-haploinsufficiency. These studies show that: 1) Notch2-haploinsufficiency limits NOD MZ B cell expansion without preventing T1D, 2) BTK supports the Notch2 pathway in NOD MZ B cells, and 3) autoreactive NOD B cell survival relies on BTK more than Notch2, regardless of MZ location, which may have important implications for disease-intervention strategies.

[1]This work was supported by NIH grant R01 DK084246 (PK), T32HL069765 (LN), and JDRF 3-2013-121 (RHB). The VMC Flow Cytometry Shared Resource is supported by the Vanderbilt Ingram Cancer Center (P30 CA68485) and the Vanderbilt Digestive Disease Research Center (DK058404). The Vanderbilt Translational Pathology Shared Resource is supported by 5U24 DK059637.

[2]Bruton's tyrosine kinase, BTK; Follicular, FO; pre-Marginal Zone, pMZ; Marginal Zone, MZ; Transitional (early), T1; Transitional (late), T2

Corresponding Author: Peggy L. Kendall, Phone: 615-322-4746, Fax: 622-322-6248, peggy.kendall@vanderbilt.edu.

Introduction

Marginal zone (MZ) B cells have increased propensity for autoreactivity. These long-lived cells reside at the outer edges of B cell follicles where they are poised to act as T-cell-independent first-responders to blood-borne antigens (1-4). The tendency of autoreactive BCRs to preferentially select into this subset, together with expanded MZs in autoimmune-prone strains of mice, drives interest in understanding their mechanisms of selection and action in autoimmune disease. In NOD mice, the MZ is enlarged and has been postulated to promote autoimmune diabetes (5-7).

Notch2 is critical for MZ B cell development (8-12). Notch2 on the B cell surface interacts with its ligand at relatively low affinity in the marginal zone sinuses (13). MZ B cells are highly dependent on these signals, as haploinsufficiency of Notch2 (*Notch2*$^{+/-}$) severely reduces this subset in C57BL/6 mice (12). Homozygous Notch2 deficiency is embryonic lethal, but B cell-targeted Notch2 deficiency (*Notch2*$^{-/-}$) reproduces MZ B cell depletion seen in *Notch2*$^{+/-}$mice, without affecting other splenic B cell compartments, localizing its primary function to this subset (8).

Autoantigen-driven selection into the MZ indicates that BCR signaling also contributes to MZ development. B cells expressing anti-insulin BCR transgenes (125Tg) illustrate this concept, as they bind antigen in vivo at all developmental stages and are disproportionally distributed to the MZ in both NOD and C57BL/6 mice (14). BCR signaling strength is a factor in MZ selection, with weaker signals favoring MZ selection and stronger signals leading to FO selection (2). However, BCR-signaling pathways important for such selection have not been well-defined. In particular, BTK, which mediates activation signals from the BCR, is known for its role in follicular B cell maturation but is generally not considered to be a participant in MZ development, except in rare cases involving transgenes that generate low affinity BCRs (2, 15-19).

Factors contributing to the increased MZ B cell compartment in NOD and other autoimmune strains are not well-understood. Recent work comparing gene expression in NOD vs. nonautoimmune MZ compartments found differences in genes controlling cell-trafficking, suggesting that factors influencing chemotaxis to the MZ also play a role (6). Components of the extracellular matrix newly discovered to contribute to MZ development are also overexpressed in the MZ of NOD mice (20). Our group has shown that polymorphisms in Igκ genes contribute to increased propensity for autoreactivity in NOD B cells and that these polymorphisms are shared with SLE-prone mice (21, 22). B cell intrinsic tolerance defects in the NOD strain also allow increased numbers of autoreactive B cells to reach maturity (22-24). These features in autoimmune-prone strains are likely to create a larger autoreactive repertoire available for selection into the MZ.

To better understand the role of MZ B cells in autoimmune diabetes, *Notch2* haploinsufficiency was introgressed onto the NOD strain with the goal of eliminating these autoreactive-prone cells, as it does in nonautoimmune strains. However, a subset of NOD MZ B cells proved resistant to this strategy. BCR-mediated signaling was found to contribute to survival of *Notch2*$^{+/-}$/NOD MZ B cells, as *Btk*-deficiency eliminated them,

while low-level BCR signaling typical of anti-insulin B cells enhanced their numbers. Furthermore, elements of the Notch2 signaling pathway had increased expression in NOD MZ B cells compared with C57BL/6 MZ B cells, and *Btk*-deficiency reduced these levels in NOD, but not C57BL/6 B cells. Studies of anti-insulin B cell clonotypes showed that BTK-dependent MZ selection and survival depend on BCR signal strength while Notch2-mediated effects do not. Finally, the ability of *Notch2* haploinsufficiency to reduce autoreactive B cell selection into the MZ does not translate into overall reduction in autoreactive cell numbers, which may have important clinical implications, as suggested by the failure of this model to protect against T1D.

Materials and Methods

Mice

Notch2$^{+/-}$ founder mice were kindly provided as a gift from James W. Thomas at Vanderbilt University, and C Klug, University of Alabama at Birmingham, with permission from Hamada, et.al, who developed them (8, 12). *Notch2*$^{+/-}$ mice were crossed with NOD mice and backcrossed for >10 generations. Offspring were homozygous for all NOD *idd* loci tested, as previously described (25) and shown in Table I. Briefly, DNA was prepared from tail biopsies using DNeasy Blood and Tissue Kit from Qiagen (cat# 69506). PCR: DNA was initialized for 5' at 94°C, then 40 cycles under the following conditions: 45s at 94°C, 45s at 53°C, and 1' for 72°C; with the exception of *idd* loci 10/3 and 5/1 in which the elongation step occurred at 72°C for 2'. A final elongation step for all loci was completed at 72°C for 7'. All samples were run on 4% NuSieve 3:1 agarose (Lonza, cat #50090) and visualized with BioRad GelDoc XR+ system. 125Tg/NOD, V_H125Tg/NOD mice and *Btk*-deficient (*Btk*^{null}) NOD mice were generated as previously described (25-27). All mice were housed in specific pathogen-free conditions, with autoclaved food and water. All studies were approved by the Vanderbilt Institutional Animal Care and Use Committee.

Disease studies

Blood glucose levels were measured weekly and mice considered diabetic at the first of two consecutive readings above 200 mg/dL.

Flow cytometry

Spleens were ground into a single cell suspension using BD Falcon cell 70μm nylon cell strainer (cat # 352350) and RBCs lysed with Tris NH_4Cl for 3 min. Cells were resuspended in 2.5% sodium azide, 5% FBS, and 2% EDTA in PBS. Staining was performed using fluorochrome- conjugated antibodies against B220 (RA3-6B2), IgD (11-26c.2a), CXCR5 (2G8), CD19 (1D9), CD21 (7G6), CD23 (B3B4) (BD Biosciences) or IgM (μ chain-specific, Life Technologies). 7 Aminoactinomycin-D (BD Biosciences) was used for the exclusion of dead cells. Insulin-binding B cells were detected with biotinylated insulin, prepared as previously described(21), followed by streptavidin-flourochrome. Inhibition studies were completed using duplicate samples to which ten-fold quantities of unlabeled insulin were added. Labeled cells were read using an LSRII flow cytometer (BD Biosciences). Data was analyzed using FlowJo software (Tree Star).

Immunofluorescence microscopy

Harvested spleens were soaked overnight in 30% sucrose and subsequently snap frozen in Tissue-Tek O.C.T. compound (Sakura Finetek). 8μm frozen sections were cut by the Vanderbilt Translational Pathology Shared Resource using a cryostat microtome (Leica). Prior to staining, sections were rehydrated briefly in 1X PBS, and then fixed for 5 min with freshly prepared 1% formaldehyde/1X PBS. Sections were blocked with 1% bovine serum albumin (BSA, Sigma)/5% normal goat serum (NGS, Life Technologies)/1X PBS. Slides were stained with the following antibodies diluted in 1% BSA/5% NGS/1X PBS: IgM-alexa488 (Life Technologies) and rat anti-mouse MOMA-1 (Cedarlane) detected with a goat anti-rat IgG-Texas Red (Southern Biotech), and then mounted using fluorescence mounting media (DAKO). An Olympus BX60 epifluorescence microscope and CCD camera controlled by MagnaFire software (Optronics International) was used for 10X image acquisition. Image contrast and brightness were adjusted using Adobe Photoshop software (Adobe Systems) to optimize the signal to noise ratio.

Quantitative real-time PCR

Splenocytes were isolated as above from wild-type or *Btk*-deficient NOD and C57BL/6 mice. Magnetic activated cell sorting (MACS) was used to deplete CD43 expressing cells using LS columns (Miltenyi). Purified cells were then stained using fluorochrome-conjugated antibodies to IgD, CD21, CD23 as above, and to IgM[b] (AF6-78). Alexa Fluor® 700 Succinimidyl Ester (Life Technologies) was used to exclude dead cells. Cells were sorted for $IgM^{int}IgD^{+}CD21^{lo}CD23^{hi}$ follicular (FO), $IgM^{hi}IgD^{lo}CD21^{hi}CD23^{lo}$ marginal zone (MZ), $IgM^{hi}IgD^{+}CD21^{lo}CD23^{hi}$ transitional 2 (T2), or $IgM^{hi}IgD^{+}CD21^{hi}CD23^{hi}$ pre-marginal zone (pMZ) B cells by fluorescence-activated cell sorting (FACS) using a BD FACSAria III cell sorter. Total RNA was isolated from each fraction using the RNeasy Micro Kit (Qiagen) and converted to cDNA as previously described(22). qRT-PCR was performed using the iCycler iQ™ Real-Time PCR Detection System (Bio-Rad) using EXPRESS SYBR® GreenER™ supermix with premixed ROX (Invitrogen). mRNA levels were normalized by the comparative cycle threshold (ΔΔCt) method, relative to hypoxanthine guanine phosphoribosyl transferase (HPRT) and reported as fold change compared to the wild-type C57BL/6 MZ B cell mean. Primers used were Hairy/enhancer of split homologue 5 (Hes5) forward 5’-GAGATGCTCAGTCCCAAGGAGAAA, reverse 5’-CGAAGGCTTTGCTGTGTTTCAGGT(28); Notch 2 forward 5’-ACATCATCACAGACTTGGTC, reverse 5’-CATTATTGACAGCAGCTGCC(29); and HPRT forward 5’-AGGTTGCAAGCTTGCTGGT, reverse 5’-TGAAGTACTCATTATAGTCAAGGGCA (Integrated DNA Technologies).

Statistical analysis

P values were calculated using Student's T test for comparisons of cell numbers or percentages. For qRT-PCR, p values were calculated using a two-way ANOVA with Sidak correction for multiple comparisons. Log-rank comparison was used for Kaplan-Meier survival curves. Values <0.05 were considered significant.

Results

Notch2 haploinsufficiency blocks MZ B cell expansion, but does not eliminate the MZ in NOD mice

Past investigations using nonautoimmune C57BL/6 with B cell-targeted *Notch2* deficiency, or global *Notch2* haploinsufficiency (*Notch2*$^{+/-}$), showed that both approaches eliminate MZ B cells (8, 12). Therefore, we introgressed *Notch2*$^{+/-}$ onto NOD mice to study selection and function of MZ B cells in the setting of autoimmunity. In contrast to studies in C57BL/6 mice, *Notch2* haploinsufficiency in NOD mice does not eliminate MZ B cells (Figure 1A-C). Rather, the MZ B cell population is reduced to levels that approach normal in nonautoimmune strains: *Notch2*$^{+/-}$/NOD had 4.98 ± 1.14% (1.32 ± 0.49 × 10^6) MZ B cells vs. 16.44% ± 0.71% (3.5 ± 1.0 × 10^6) for WT NOD ($p < 0.001$ for both percentage and total numbers). Of note, MZ B cell normalization had no effect on CD4 or CD8 T cell numbers (Supplemental Table 1.) To assess whether the MZ B cells identified by flow cytometry in *Notch2*$^{+/-}$/NOD are anatomically positioned in the marginal zone, immunofluorescence microscopy was used to detect B cells outside the metallophilic macrophage ring that delineates the MZ. White arrows in representative images depict B cells (IgM$^+$, green) outside the metallophilic macrophage ring (MOMA-1$^+$, red) in NOD and *Notch2*$^{+/-}$/NOD mice (Fig. 1D). *Notch2*$^{+/-}$/NOD images are similar to our previously published data regarding C57BL/6 marginal zones (14) and show that B cells retain the ability to traffic to the MZ in *Notch2*$^{+/-}$/NOD mice.

Normalization of MZB compartment size does not protect against diabetes

To determine whether reduction of MZ B cell numbers prevents diabetes development, we performed a disease study on female *Notch2*$^{+/-}$/NOD and WT NOD littermates. As shown in Figure 1E, haploinsufficiency of *Notch2* does not confer disease protection, as more than 70% of mice in both groups become diabetic by 30 weeks of age. Thus, reversal of the abnormal expansion of the MZ found in NOD mice is insufficient to protect against diabetes development.

Insulin-specific NOD B cells maintain supranormal MZ B cell numbers in Notch2 haploinsufficiency

Insulin specificity conferred by a transgenic BCR (125Tg) produces an enlarged MZ B cell compartment in C57BL/6 mice, illustrating the contribution of BCR-mediated antigen selection in directing B cells to the MZ compartment. This specificity further expands the MZ B cell compartment in NOD mice (14). To examine the interplay between this autoreactive BCR specificity and Notch2 in the development of the MZ, we crossed 125Tg mice with *Notch2*$^{+/-}$ on both B6 and NOD backgrounds. As shown in Figure 2A, 125Tg B cells bind insulin specifically (left panels), and this is not altered by haploinsufficiency of Notch2 (right panels), nor is the total number of anti-insulin B cells reduced (36.3 ± 11.1 × 10^6 vs. 42.0 ± 6.6 × 10^6, $p = 0.37$). The percent of MZ B cells in 125Tg/NOD and 125Tg/B6 is 51.7 ± 9.9% and 37.45 ± 7.95% of total B cells respectively (Figure 2C). On the nonautoimmune, B6 background, this expanded anti-insulin MZ is significantly reduced, but not eliminated by Notch2 insufficiency, with 8.02 ± 3.98% of B cells retaining the MZ phenotype (Figure 2C). On the NOD background however, 125Tg/*Notch2*$^{+/-}$/NOD B cells

are still highly capable of maintaining a large MZ compartment, comprising 31.5 ± 3.3% of total B cells (Figure 2B and Figure 2C). Total numbers of MZ B cells follow this same trend, as shown in Figure 2D. Overall, B6 MZ anti-insulin B cells are more dependent on Notch2 than NOD B cells are, as 125Tg/*Notch2*$^{+/-}$/NOD MZB cells are reduced by less than half compared with their 125Tg/NOD counterparts, while numbers of 125Tg/*Notch2*$^{+/-}$/B6 MZB cells are reduced more than 5-fold (Figure 2E). Thus, both autoreactive BCR specificity, and the presence of an autoimmune background, can override the exquisite dependence on Notch2 exhibited by MZ B cells in C57BL/6 mice with endogenous BCRs.

Bruton's tyrosine kinase is required by MZ B cells in Notch2$^{+/-}$/NOD mice

The ability of autoreactive (anti-insulin) B cells to continue to enter the MZ in *Notch2*$^{+/-}$/NOD mice suggested that BCR-mediated signaling allows some NOD MZ B cells to overcome Notch2 haploinsufficiency. To test the hypothesis that BCR-mediated signaling supports the MZ compartment that remains in *Notch2*$^{+/-}$/NOD mice, we crossed *Btk*-deficient NOD mice with *Notch2*$^{+/-}$/NOD mice. As shown in Figure 3, the MZ B cell compartment in *Btk*-deficient *Notch2*$^{+/-}$/NOD mice is obliterated ($0.11 \pm 0.04 \times 10^6$ vs. *Notch2*$^{+/-}$/NOD $1.28 \pm 0.48 \times 10^6$, $p < 0.01$), similar to the effects of Notch2 haploinsufficiency alone in C57BL/6 mice. This contrasts with total numbers of B cells, which show no statistically significant difference conferred by the loss of BTK in *Notch2*$^{+/-}$/NOD mice ($12.1 \pm 3.3 \times 10^6$ vs. $9.3 \pm 2.3 \times 10^6$, $p = 0.16$). These findings indicate that selection into the enlarged MZ of NOD mice relies on both Notch2 and BTK-mediated signaling. Of note, the *Btk*-deficient *Notch2*$^{+/-}$/NOD model is not suitable for analysis of MZ contribution to disease outcome as *Btk*-deficient NOD are already disease-protected, and have other B cell abnormalities such as signaling defects and an absent B1a compartment (25).

BTK supports elevated Notch2 expression and signaling in the NOD marginal zone compartment

The observation that BTK supports the development of the marginal zone suggests that BCR-mediated signaling may support the Notch2 signaling pathway in NOD mice. To determine the effect of BTK loss on the expression of *Notch2* and its targets, we isolated B cells from wild type or *Btk*-deficient NOD mice and sorted them into FO, MZ, T2, and pMZ subsets (Figure 4, A-B). B cell subsets from WT and *Btk*-deficient C57BL/6 mice were also analyzed to determine potential differences conferred by the two genetic backgrounds. Total RNA was isolated from each subset and reverse transcribed to generate cDNA. Real time PCR was then used to analyze levels of *Notch2* and its transcriptional target, *Hes5*. Ct values were normalized to *HPRT* transcript levels for each sample and relative values for all subsets were compared. *Notch2* levels were strikingly increased in WT NOD compared to WT B6 in the MZ ($p < 0.0001$) and pMZ ($p < 0.0001$) cell subsets. *Hes5* expression, in parallel, was significantly increased in the WT NOD MZ compared to WT B6 MZ ($p = 0.0081$). *Notch2* transcripts were found to be significantly decreased ($p = 0.0012$) in the pMZ compartment of *Btk*^{null} NOD mice as compared to WT NOD controls (Figure 4C). Accordingly, transcript levels of *Hes5* were significantly decreased ($p = 0.0413$) in the MZ compartment of *Btk*^{null} NOD mice, and a trend of decreased transcript levels is observed across all subsets compared to wild-type controls. In contrast, no significant difference was

seen between WT B6 and *Btk*^{null} B6. In addition, no difference was seen in *Notch2* or *Hes5* expression in FO B cells from any of the four groups (B6 vs. NOD vs. *Btk*^{null} B6 vs. *Btk*^{null} NOD, not shown), nor was there a significant difference in *Notch2* expression between preMZ vs. MZ in C56BL/6. These data suggest that BCR signaling, mediated by BTK, promotes the development of the MZ by supporting increased *Notch2* expression in pMZ NOD B cells, with downstream effects on Notch2 transcriptional activity that is most significant in MZ B cells. However, this effect is only seen in the NOD, which exhibits significantly more Notch2 transcription than the B6.

BTK-mediated support of MZ B cells depends on the quality of BCR-antigen interactions

Anti-insulin B cells expressed in the 125Tg model rely on both H chain and L chain transgenes, and are critically dependent on BTK as they fail to mature into either MZ or FO cells in its absence (30). Expression of the HC transgene alone (V_H125) generates a broad repertoire in which endogenous light chains pair with the V_H125Tg (21, 31, 32). In NOD, but not C57BL/6 mice, two of these L chains generate insulin-binding BCRs that enter the mature repertoire (22). As shown in Figure 5A, V_H125Tg/NOD B cells expressing these two L chains can be visualized by flow cytometry as two independent populations. As we previously reported, Vκ4-74 is found paired with V_H125 in the population with a higher MFI, while cells expressing Vκ4-57-1 is found in the lower MFI population (22). However, this flow cytometry analysis was performed using human insulin. When these antibodies were produced and tested in ELISA-based comparisons of rodent versus human insulin binding, V_H125/Vκ4-57-1 (Low MFI) was found to bind rodent insulin comparatively better than V_H125/Vκ4-74 (High MFI) (22). This suggests greater occupancy of the V_H125/Vκ4-57-1 with endogenous rodent insulin, resulting in poorer competition for binding by the labeled human insulin, with a lower MFI as a result. Thus, these populations are referred to as high autoreactive (High Auto, V_H125/Vκ4-57-1, Low MFI) and low autoreactive (Low Auto, V_H125/Vκ4-74, High MFI) to indicate their differences in autoreactivity with endogenous rodent insulin. As shown in Figure 5B, the cells that bind rodent insulin less well (Low Auto) are preferentially selected into the MZ compared to those that bind rodent insulin better. (Low Auto MZB: $1.9 \pm 0.47 \times 10^5$ vs. High Auto MZB: $1.0 \pm 0.45 \times 10^5$ cells, $p = 0.002$). High autoreactive B cells are evenly distributed between MZ and FO compartments and are found in the FO compartment in equivalent numbers to the cells with low autoreactivity. (Low Auto FO: $0.72 \pm 0.17 \times 10^5$ vs. High Auto FO: $0.79 \pm 0.33 \times 10^5$ cells $p = 0.6$). To determine the effects of BCR-mediated signaling on these two insulin-binding populations, *Btk*-deficient (*Btk*^{null}) V_H125/NOD mice were used (25). This model has an H chain transgene effect that confers some reduction to all *Btk*-deficient V_H125/NOD B cells. We previously reported that the total number of insulin-binding cells is significantly reduced in this model (25), and here report how the insulin-binding L chain and compartment localization affect their BTK-dependency. As shown in Figure 5C, Low Auto MZ B cells are very sensitive to loss of BTK, beyond the effect seen in these cells in the FO/T2 compartment, or when compared to overall B cell loss in the general repertoire. High Auto B cells, on the other hand, are not disproportionally reduced in the MZ any more than the overall B cell repertoire. In the FO compartment, all insulin-binding B cells are slightly reduced compared with the overall B cell reduction, but the greatest loss of anti-insulin B cells comes from the Low Auto MZ B cell population.

Notch2-haploinsufficiency shifts anti-insulin B cells away from the MZ, independent of autoreactivity, but does not reduce their total numbers

To determine the Notch2 dependence of differentially autoreactive anti-insulin B cells, we next crossed Notch2 haploinsufficiency onto the V_H125Tg/NOD model (Fig. 6). The percentages of both Low and High Autoreactive populations that distributed into the MZ were greatly reduced in V_H125Tg/*Notch2*$^{+/-}$/NOD (High Auto MZ: 14.7 ± 12 % vs. 46.7 ± 15.7%, $p < 0.001$. Low Auto MZ: 11.7 ± 7.4% vs. 40.9 ± 22.2 %, $p = 0.002$. Fig. 6B). Conversely, the percentages of anti-insulin B cells in the T2/FO compartment were increased in V_H125Tg/*Notch2*$^{+/-}$/NOD (High Auto T2/FO: 77.5 ± 12.5% vs. 47.6 ± 12.9%, $p < 0.001$. Low Auto T2/FO: 77.7 ± 8.7 % vs. 51.4 ± 18.6% $p = 0.002$, Fig. 6B). The percentages of non-insulin-binding B cells in the V_H125Tg/*Notch2*$^{+/-}$/NOD mice were also reduced in the MZ compartment (10.6 ± 3.1% vs. 40.9 ± 11.5%, $p < 0.001$) and increased in the T2/FO compartment (79.1 ± 5.0% vs. 51.7 ± 8.5%, $p < 0.001$, Fig. 6B). The reduced MZ percentage in V_H125Tg/*Notch2*$^{+/-}$/NOD mice was reflected in decreased numbers of anti-insulin MZ B cells in both the Low and High Auto populations (High Auto MZ: 6.0 ± 4.9 × 10^3 vs. 24.2± 18.1 × 10^3, $p = 0.015$. Low Auto MZ: 4.9 ± 3.0 × 10^3 vs. 29.8 ± 29.4 × 10^3, $p = 0.03$), as well as in numbers of non-insulin-binding MZ B cells (681 ± 249 × 10^3 vs. 4863 ± 3441 × 10^3, $p = 0.004$, Fig. 6C). The average numbers of High Auto anti-insulin B cells in the T2/FO compartment were increased (44.3 × 10^3 vs. 20.8 × 10^3, $p = 0.04$). The average numbers of Low Auto T2/FO B cells (40.3 × 10^3 vs. 29.6 × 10^3, $p = 0.23$) or non-insulin-binding T2/FO B cells (5341 × 10^3 vs. 5365 × 10^3) were not different. Overall, total insulin-binding B cell numbers were not significantly different in *Notch2*$^{+/-}$ vs. *Notch2*$^{+/+}$ V_H125Tg/NOD mice (89.1 ± 43.0 vs. 110.6 ± 61.7 × 10^3 $p = 0.42$). These data show that Notch2 haploinsufficiency reduces insulin-binding B cells in the MZ, but does not preferentially impact the Low Autoreactive population, nor decrease the overall numbers of these autoreactive cells.

Discussion

The enlarged MZ B cell compartment in NOD mice has been implicated in type 1 diabetes development, but the mechanisms underlying this expansion have not been not well-understood (5). The studies presented here show that NOD MZ B cells are surprisingly less reliant on Notch2 than their C57BL/6 counterparts. While *Notch2*$^{+/-}$/C57BL/6 mice have very few MZ B cells, *Notch2*$^{+/-}$/NOD retain a robust MZ (Figures 1 and 2). In accordance with these findings, analysis of transcript expression of *Notch2*, and its downstream target *Hes5*, show that they are more highly expressed in NOD MZ cells than in C57BL/6 MZ cells (Fig. 4), suggesting that the single allele remaining in the *Notch2*$^{+/-}$/NOD model provides enough signal to drive development of a MZ commensurate in size with WT C57BL/6. This relative normalization of numbers of MZ B cells in *Notch2*$^{+/-}$/NOD mice does not reduce diabetes, however, indicating that numeric expansion of this compartment is not a primary driving factor in diabetes development (Fig 1). Surprisingly, we find that increased *Notch2* found in NOD mice relies on BTK, as *Btk*-deficiency reduces *Notch2* overexpression in NOD cells, without having any effect in the nonautoimmune setting (Fig. 4). Likewise, *Notch2*$^{+/-}$/NOD MZ B cells are highly dependent upon BTK, again differing from nonautoimmune mice, in which loss of BTK mainly affects the follicular compartment

((16)and Fig 3). These data provide a direct link between BTK and Notch2 in the NOD model, and suggest that BCR-mediated signaling interacts with the Notch2 pathway for selection and maintenance of NOD MZ B cells. This idea is reinforced by studies using anti-insulin B cell transgenes to show that BCR specificities contribute to MZ selection and are fine tuned in their reliance on BTK, as one V_H125 clonotype is reduced by BTK deficiency while the other is not (Fig 5). Finally, these transgenes also reveal that impairment of Notch2 shifts autoreactive cells out of the MZ but does not eliminate them, leaving them available to participate in T1D. Future studies using B cell-specific homozygous depletion of Notch2 in NOD mice would be useful in further evaluating both the dependency of NOD MZ B cells on Notch2 and their role in the disease process.

Notch2 contribution to MZ development in nonautoimmune strains has been demonstrated using both global genetic haploinsufficiency and B cell specific homozygous deficiency. Studies using *Notch2*$^{+/-}$/C57BL/6 mice showed near-complete elimination of the MZ (12), as did those with B cell-specific homozygous deletion, with no further effects on B cells (8). These comparable phenotypes seemed to indicate that MZ B cells are so dependent upon Notch2 that even partial depletion by haploinsufficiency can block their development as well as full genetic ablation does. However, this may not be the case in autoimmune strains. Our data are complementary to previous work showing that blockade of the Notch ligand Delta-like 1 eliminated the MZ in C57BL/6, while a similarly enlarged MZ in lupus-prone BWF mice were partially resistant to this treatment (33). The findings reported here suggest that *Notch2* overexpression in NOD B cells, driven by BCR-mediated signaling, underlies the increased MZ in this autoimmune strain, and is the most likely reason for its resistance to depletion using haploinsufficiency.

Alterations in cell trafficking have also been implicated in MZ differences between NOD and nonautoimmune strains (6). Because of this, we also tested surface levels of the homeostatic B cell chemokine receptor, CXCR5, in *Notch2*$^{+/-}$/NOD vs. WT NOD and C57BL/6, but saw no differences (Supplemental Figure 1). Nevertheless, many other chemotactic factors and integrins could play a role, and deserve future study. Of note, the same report, which relied on microarray to assess differences, did not reveal the *Notch2* overexpression that we found using qRT-PCR. The reason for this is not clear, but could be due either to variability between the assays, with qRT-PCR being more sensitive, or in the cell sorting method. We found that sorting into subsets that differentiated between T2 and follicular, as well as preMZ and MZ was helpful in identifying differences, whereas broader, more heterogeneous categories were less sensitive for these purposes, and may miss nuances between subsets.

Cell signaling responses that drive MZ B cell development, selection, and support are complex and incompletely understood, even in nonautoimmune mice. Integration of signals from the BCR with Notch2, BAFFr, and various chemokine receptors contribute, as do components of the extracellular matrix (2, 6, 20). The classic model of MZ B cell selection and development suggests that low affinity, or weak, BCR signals mediate MZ B cell selection in a BAFFr- and BTK-independent manner, while stronger, tonic signals mediated by BAFFr and BTK, drive follicular B cell development. Multiple studies have shown that MZ B cells with endogenous BCRs in nonautoimmune strains do not require BTK (16, 17).

Therefore, we were surprised to find that loss of BTK almost completely eliminated the NOD MZ compartment that remained in *Notch2*$^{+/-}$/NOD mice. Our previous studies showed a small, but statistically significant decrease in MZ B cells in *Btk*-deficient NOD mice, with concomitant increase in pre-MZ cells, indicating a partial block in maturation (25). Our new findings show that loss of BTK also significantly reduces *Notch2* transcript expression in pMZ NOD B cells, and significantly decreases its transcriptional target, *Hes5*, in MZ B cells (Fig. 4), indicative of loss of function that is consistent with the block at the pMZ stage and decreased MZ, in these mice. Interestingly, *Hes5* expression differences lag behind *Notch2* expression differences in these models, trending downward in BTK-deficient NOD preMZ but not becoming statistically significantly different from WT NOD until the MZ stage. At the same time, *Notch2* expression, while still trending lower than WT NOD, loses statistical significance at the MZ stage. Since this assay measures transcripts, rather than protein, this may reflect altered surface Notch2 protein expression, or its rapid turnover in the absence of BTK. Of note, pre-MZ in C57BL/6 have a similar disconnect between *Notch2* transcript expression, which is quite low, and *Hes5*, which does not differ significantly from NOD at this stage. Again this may indicate that surface levels of the Notch2 protein are adequate, reducing further transcription in B6 pMZ B cells. Overall, these combined discoveries suggest that selection of some NOD B cells into the MZ depends on BTK, contrasting classic characteristics of MZ B cells in nonautoimmune strains.

Direct crosstalk between BTK-mediated pathways and those of Notch2 have not been shown before. In fact, it has been postulated that BTK might function as a negative regulator of factors that drive MZ development (34). A classic study showed lack of this compartment in mice deficient for Aiolos, a negative regulator. When BTK deficiency (*xid*) was used to balance Ailos deficiency, the MZ was restored (15). However, this same strategy failed to reverse the reduced MZ compartment found in NF-κB1/p50 mice, and in fact further decreased MZ numbers, although this was not statistically significant (34). This same report showed that NF-κB1/p50 also supports expression of both *Hes5* and *Deltex1*, transcriptional targets of Notch2. Thus, the NF-κB pathway, a downstream target of BTK-mediated signaling, seems a likely candidate for linking BTK with Notch2 in some models, and in fact, NF-κB has been shown to have increased activity in NOD B cells, further supporting this concept (35).

Of note, we also tested potential effects of *Notch2* haploinsufficiency on BCR-mediated signaling, including phosphorylation of Syk, BLNK and PLCγ2, and found no differences (Supplemental Figure 2). CD19 provides support for activating signals, is more highly expressed in NOD B cells and has been linked to MZ development, but examination of *Notch2*$^{+/-}$/NOD B cells showed no alteration in CD19 expression compared to WT NOD (Supplemental Figure 1). Thus, while BTK appears to support the Notch2 pathway in NOD B cells, we did not find evidence of the reverse.

Two recent additional studies, when taken together, also support the idea that BTK may negatively regulate Notch2 via the transcription factor IRF4 in nonautoimmune mice. One of these showed that inducible B cell-specific deletion of *Irf4* increased Notch2 expression and caused accumulation of B cells in the MZ (28). A second study showed that the BTK-

inhibitor Ibrutinib decreases IRF4 expression, which is responsive to BCR signaling effects (36). These combined findings would predict that BTK deficiency should decrease IRF4 expression, which in turn should increase Notch2 and MZ B cells, the opposite of our experimental results. Several differences in the experimental models could account for this unexpected outcome. IRF4 has various functions that are context dependent, and graded, in both normal B cells and B cell tumors. The Ibrutinib studies were performed on human activated B cell like diffuse large B cell lymphoma cell lines, in which IRF4 expression is increased in response to continuous BCR signaling resulting from mutations of proteins in the signaling pathway. These circumstances likely do not reflect events during development in normal murine B cells. Similarly, the B cell inducible *Irf4*$^{-/-}$ model provides insight into IRF4 actions in mature C57BL/6 B cells, producing Notch2 effects within an established, mature, B cell milieu. In contrast, *Btk*-deficiency in the *Notch2*$^{+/-}$/NOD model affects B cells throughout the life cycle and shows that decreased BTK-mediated signaling in developing and mature B cells does not induce increased MZ B cell development. Finally, NOD B cells used here may also have subtle differences in signaling responses that would contribute to different outcomes from that in human tumor cells or murine B cells from nonautoimmune mice.

Because BTK contributes to both BCR and BAFFr signaling (37, 38), it is possible that both pathways may be affected in this process. However, the dependence of one, but not both, anti-insulin populations on BTK in the V_H125 model indicates that BCR-mediated signaling is a critical component. In this model, two insulin-binding populations are generated by different endogenous L chains that pair with the anti-insulin transgenic H chain (Fig 5). Anti-insulin B cells with relatively lower rodent insulin binding (22) are preferentially selected into the MZ and depend upon BTK, as their numbers are reduced by its genetic ablation (Fig. 5). This contrasts those with higher relative rodent insulin binding, which are evenly distributed between MZ and FO and are not numerically reduced by loss of BTK. These differing outcomes based on specificity may also contribute to a previously published model using an anti-DNA transgenic BCR, 56R, which was determined to rely on BTK for MZ localization, but not survival(19). Of note, anti-insulin 125Tg B cells (in which both anti-insulin H and L chain transgenes are expressed, Fig. 2) are highly dependent on BTK, and both FO and MZ B cells are depleted by greater than 95%, regardless of background strain (30). Thus, fine-tuned differences in BCR specificity affect reliance on BTK for MZ selection, and further affects reliance on BTK for survival. B cells from autoimmune-prone mice have altered signaling thresholds, which reduce tolerance and generate increased numbers of BCRs with specificities that may be suitable for entry into the MZ (21, 22, 24). This may simply provide a numeric advantage that allows discernment of a partial effect of Notch2 haploinsufficiency that may be present, but less visible, in strains with smaller MZs. The effect of this property is seen in the anti-insulin BCR transgenic model (Fig. 2), in which the MZ is expanded on both B6 and NOD models, and shows partial resistance to elimination by *Notch2*-haploinsufficiency. Such a mechanism may also be represented by the TgV_H3B4 model, developed from a “natural,” polyreactive antibody, which generates an enlarged MZ. These mice also maintained a small MZ in the absence of the Notch downstream transcription factor RBP-J, despite being on the C57BL/6 background (39). Thus, in both of these models, transgenic B cells with autoreactive specificities were more

likely to enter the MZ, and to be partially resistant to impairment in Notch2 signaling even on a nonautoimmune background, confirming that increased numbers of autoreactive B cells can affect Notch2-dependence. Importantly, the anti-insulin 125Tg studies presented here provide an opportunity to evaluate effects of BCR-specificity and the NOD genetic background concurrently. As shown in Figure 2, anti-insulin B cells make up more than 95% of splenic B cells in this model, providing a uniform population for study across models. These autoreactive cells are more likely to go to the MZ and to be partially Notch2-independent in both models, showing the importance of BCR-mediated signaling in this process. However, in NOD mice there is clearly an additional effect that transcends BCR specificity, as 125Tg/NOD have very exaggerated MZ populations, comprising about half of B cells in NOD mice, and nearly a third even in *Notch2*$^{+/-}$/NOD mice. Therefore these studies show clearly that both BCR specificity and other aspects of the NOD background contribute to the enlarged MZ seen in NOD mice.

Overall, our data show that the enlarged MZ B cell compartment in NOD mice has reduced dependence on Notch2, and an unexpected dependence on BTK, that contrasts with nonautoimmune C57BL/6. Use of anti-insulin transgenic B cell models also shows that contributions of BCR-mediated signaling and BTK-dependence rely on the quality of BCR interactions with antigen. Of potential clinical importance is the finding that impairment in BTK mediated signaling reduces total numbers of anti-insulin B cells, while Notch2 impairment shifts cells out of the MZ, but does not significantly reduce autoreactive cell numbers. These findings contribute to a growing body of literature defining the complexity underlying development of this autoimmune-prone subset of cells. Future development of methods to specifically eliminate the MZ subset in NOD mice are needed to better understand the contributions of these cells to autoimmune disease.

Supplementary Material

Refer to Web version on PubMed Central for supplementary material.

Acknowledgements

We would like to acknowledge Dr. James W. Thomas, Vanderbilt University, for helpful review of the manuscript, and Dr. Wasif Khan, who developed and characterized the original BTK-deficient/C57Bl/6 model from which BTK-deficient NOD mice were derived. Flow Cytometry data acquisition was performed in the VMC Flow Cytometry Shared Resource. Frozen tissue sections were prepared by the VMC Translational Pathology Shared Resource.

References

1. Lopes-Carvalho T, Kearney JF. Development and selection of marginal zone B cells. Immunol Rev. 2004; 197:192–205. [PubMed: 14962196]
2. Pillai S, Cariappa A. The follicular versus marginal zone B lymphocyte cell fate decision. Nat Rev Immunol. 2009; 9:767–777. [PubMed: 19855403]
3. Attanavanich K, Kearney JF. Marginal zone, but not follicular B cells, are potent activators of naive CD4 T cells. J Immunol. 2004; 172:803–811. [PubMed: 14707050]
4. Foote JB, Kearney JF. Generation of B cell memory to the bacterial polysaccharide alpha-1,3 dextran. J Immunol. 2009; 183:6359–6368. [PubMed: 19841173]

5. Marino E, Batten M, Groom J, Walters S, Liuwantara D, Mackay F, Grey ST. Marginal-zone B-cells of nonobese diabetic mice expand with diabetes onset, invade the pancreatic lymph nodes, and present autoantigen to diabetogenic T-cells. Diabetes. 2008; 57:395–404. [PubMed: 18025414]
6. Stolp J, Marino E, Batten M, Sierro F, Cox SL, Grey ST, Silveira PA. Intrinsic molecular factors cause aberrant expansion of the splenic marginal zone B cell population in nonobese diabetic mice. J Immunol. 2013; 191:97–109. [PubMed: 23740954]
7. Bashratyan R, Sheng H, Regn D, Rahman MJ, Dai YD. Insulinoma-released exosomes activate autoreactive marginal zone-like B cells that expand endogenously in prediabetic NOD mice. Eur J Immunol. 2013; 43:2588–2597. [PubMed: 23817982]
8. Saito T, Chiba S, Ichikawa M, Kunisato A, Asai T, Shimizu K, Yamaguchi T, Yamamoto G, Seo S, Kumano K, Nakagami-Yamaguchi E, Hamada Y, Aizawa S, Hirai H. Notch2 is preferentially expressed in mature B cells and indispensable for marginal zone B lineage development. Immunity. 2003; 18:675–685. [PubMed: 12753744]
9. Tanigaki K, Han H, Yamamoto N, Tashiro K, Ikegawa M, Kuroda K, Suzuki A, Nakano T, Honjo T. Notch-RBP-J signaling is involved in cell fate determination of marginal zone B cells. Nat Immunol. 2002; 3:443–450. [PubMed: 11967543]
10. Hozumi K, Negishi N, Suzuki D, Abe N, Sotomaru Y, Tamaoki N, Mailhos C, Ish-Horowicz D, Habu S, Owen MJ. Delta-like 1 is necessary for the generation of marginal zone B cells but not T cells in vivo. Nat Immunol. 2004; 5:638–644. [PubMed: 15146182]
11. Hampel F, Ehrenberg S, Hojer C, Draeseke A, Marschall-Schroter G, Kuhn R, Mack B, Gires O, Vahl CJ, Schmidt-Supprian M, Strobl LJ, Zimber-Strobl U. CD19-independent instruction of murine marginal zone B-cell development by constitutive Notch2 signaling. Blood. 2011; 118:6321–6331. [PubMed: 21795747]
12. Witt CM, Won WJ, Hurez V, Klug CA. Notch2 haploinsufficiency results in diminished B1 B cells and a severe reduction in marginal zone B cells. J Immunol. 2003; 171:2783–2788. [PubMed: 12960298]
13. Tan JB, Xu K, Cretegny K, Visan I, Yuan JS, Egan SE, Guidos CJ. Lunatic and manic fringe cooperatively enhance marginal zone B cell precursor competition for delta-like 1 in splenic endothelial niches. Immunity. 2009; 30:254–263. [PubMed: 19217325]
14. Acevedo-Suarez CA, Hulbert C, Woodward EJ, Thomas JW. Uncoupling of anergy from developmental arrest in anti-insulin B cells supports the development of autoimmune diabetes. J.Immunol. 2005; 174:827–833. [PubMed: 15634904]
15. Cariappa A, Tang M, Parng C, Nebelitskiy E, Carroll M, Georgopoulos K, Pillai S. The follicular versus marginal zone B lymphocyte cell fate decision is regulated by Aiolos, Btk, and CD21. Immunity. 2001; 14:603–615. [PubMed: 11371362]
16. Khan WN, Alt FW, Gerstein RM, Malynn BA, Larsson I, Rathbun G, Davidson L, Muller S, Kantor AB, Herzenberg LA. Defective B cell development and function in Btk-deficient mice. Immunity. 1995; 3:283–299. [PubMed: 7552994]
17. Hardy RR, Hayakawa K, Parks DR, Herzenberg LA. Demonstration of B-cell maturation in X-linked immunodeficient mice by simultaneous three-colour immunofluorescence. Nature. 1983; 306:270–272. [PubMed: 6358897]
18. Kanayama N, Cascalho M, Ohmori H. Analysis of marginal zone B cell development in the mouse with limited B cell diversity: role of the antigen receptor signals in the recruitment of B cells to the marginal zone. J Immunol. 2005; 174:1438–1445. [PubMed: 15661902]
19. Halcomb KE, Musuka S, Gutierrez T, Wright HL, Satterthwaite AB. Btk regulates localization, in vivo activation, and class switching of anti-DNA B cells. Mol Immunol. 2008; 46:233–241. [PubMed: 18849077]
20. Song J, Lokmic Z, Lammermann T, Rolf J, Wu C, Zhang X, Hallmann R, Hannocks MJ, Horn N, Ruegg MA, Sonnenberg A, Georges-Labouesse E, Winkler TH, Kearney JF, Cardell S, Sorokin L. Extracellular matrix of secondary lymphoid organs impacts on B-cell fate and survival. Proc Natl Acad Sci U S A. 2013; 110:E2915–2924. [PubMed: 23847204]
21. Henry RA, Kendall PL, Woodward EJ, Hulbert C, Thomas JW. Vkappa polymorphisms in NOD mice are spread throughout the entire immunoglobulin kappa locus and are shared by other autoimmune strains. Immunogenetics. 2010; 62:507–520. [PubMed: 20556377]

22. Henry-Bonami RA, Williams JM, Rachakonda AB, Karamali M, Kendall PL, Thomas JW. B lymphocyte “original sin” in the bone marrow enhances islet autoreactivity in type 1 diabetes-prone nonobese diabetic mice. J Immunol. 2013; 190:5992–6003. [PubMed: 23677466]

23. Silveira PA, Dombrowsky J, Johnson E, Chapman HD, Nemazee D, Serreze DV. B cell selection defects underlie the development of diabetogenic APCs in nonobese diabetic mice. J Immunol. 2004; 172:5086–5094. [PubMed: 15067092]

24. Quinn WJ III, Noorchashm N, Crowley JE, Reed AJ, Noorchashm H, Naji A, Cancro MP. Cutting edge: impaired transitional B cell production and selection in the nonobese diabetic mouse. J Immunol. 2006; 176:7159–7164. [PubMed: 16751358]

25. Kendall PL, Moore DJ, Hulbert C, Hoek KL, Khan WN, Thomas JW. Reduced diabetes in btk-deficient nonobese diabetic mice and restoration of diabetes with provision of an anti-insulin IgH chain transgene. Journal of immunology. 2009; 183:6403–6412.

26. Hulbert C, Riseili B, Rojas M, Thomas JW. B cell specificity contributes to the outcome of diabetes in nonobese diabetic mice. J Immunol. 2001; 167:5535–5538. [PubMed: 11698422]

27. Rojas M, Hulbert C, Thomas JW. Anergy and not clonal ignorance determines the fate of B cells that recognize a physiological autoantigen. J Immunol. 2001; 166:3194–3200. [PubMed: 11207272]

28. Simonetti G, Carette A, Silva K, Wang H, De Silva NS, Heise N, Siebel CW, Shlomchik MJ, Klein U. IRF4 controls the positioning of mature B cells in the lymphoid microenvironments by regulating NOTCH2 expression and activity. J Exp Med. 2013; 210:2887–2902. [PubMed: 24323359]

29. Ellinghaus U, Rupec RA, Pabst O, Ignatius R, Forster R, Dorken B, Jundt F. IkappaBalpha is required for marginal zone B cell lineage development. Eur J Immunol. 2008; 38:2096–2105. [PubMed: 18604869]

30. Bonami RH, Sullivan AM, Case JB, Steinberg HE, Hoek KL, Khan WN, Kendall PL. Bruton's Tyrosine Kinase Promotes Persistence of Mature Anti-Insulin B Cells. J Immunol. 2014; 192:1459–1470. [PubMed: 24453243]

31. Kendall PL, Yu G, Woodward EJ, Thomas JW. Tertiary lymphoid structures in the pancreas promote selection of B lymphocytes in autoimmune diabetes. J Immunol. 2007; 178:5643–5651. [PubMed: 17442947]

32. Woodward EJ, Thomas JW. Multiple germline kappa light chains generate anti-insulin B cells in nonobese diabetic mice. J Immunol. 2005; 175:1073–1079. [PubMed: 16002708]

33. Moriyama Y, Sekine C, Koyanagi A, Koyama N, Ogata H, Chiba S, Hirose S, Okumura K, Yagita H. Delta-like 1 is essential for the maintenance of marginal zone B cells in normal mice but not in autoimmune mice. Int Immunol. 2008; 20:763–773. [PubMed: 18381350]

34. Moran ST, Cariappa A, Liu H, Muir B, Sgroi D, Boboila C, Pillai S. Synergism between NF-kappa B1/p50 and Notch2 during the development of marginal zone B lymphocytes. J Immunol. 2007; 179:195–200. [PubMed: 17579038]

35. Wheat W, Kupfer R, Gutches DG, Rayat GR, Beilke J, Scheinman RI, Wegmann DR. Increased NF-kappa B activity in B cells and bone marrow-derived dendritic cells from NOD mice. Eur J Immunol. 2004; 34:1395–1404. [PubMed: 15114673]

36. Yang Y, Shaffer AL 3rd, Emre NC, Ceribelli M, Zhang M, Wright G, Xiao W, Powell J, Platig J, Kohlhammer H, Young RM, Zhao H, Yang Y, Xu W, Buggy JJ, Balasubramanian S, Mathews LA, Shinn P, Guha R, Ferrer M, Thomas C, Waldmann TA, Staudt LM. Exploiting synthetic lethality for the therapy of ABC diffuse large B cell lymphoma. Cancer Cell. 2012; 21:723–737. [PubMed: 22698399]

37. Petro JB, Rahman SM, Ballard DW, Khan WN. Bruton's tyrosine kinase is required for activation of IkappaB kinase and nuclear factor kappaB in response to B cell receptor engagement. J Exp.Med. 2000; 191:1745–1754. [PubMed: 10811867]

38. Shinners NP, Carlesso G, Castro I, Hoek KL, Corn RA, Woodland RT, Scott ML, Wang D, Khan WN. Bruton's tyrosine kinase mediates NF-kappa B activation and B cell survival by B cell-activating factor receptor of the TNF-R family. J Immunol. 2007; 179:3872–3880. [PubMed: 17785824]

39. Zhang Z, Zhou L, Yang X, Wang Y, Zhang P, Hou L, Hu X, Xing Y, Liu Y, Li W, Han H. Notch-RBP-J-independent marginal zone B cell development in IgH transgenic mice with VH derived from a natural polyreactive antibody. PLoS One. 2012; 7:e38894. [PubMed: 22719978]

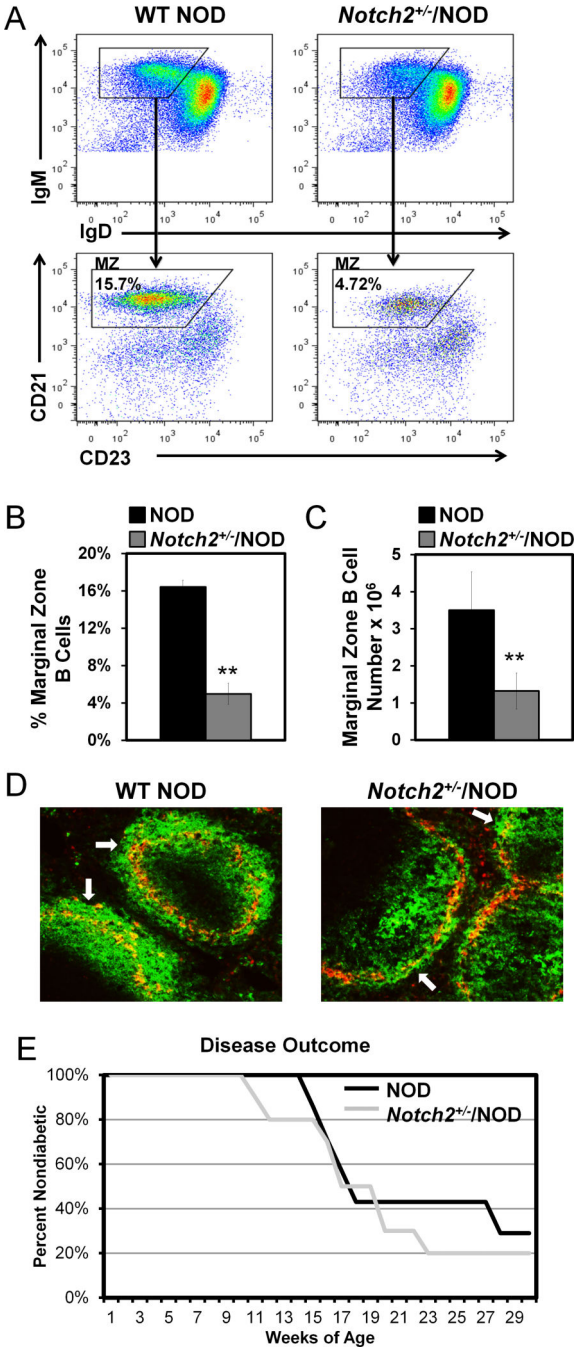

Figure 1. Notch2 haploinsufficiency corrects the expanded NOD MZ compartment, but does not protect against diabetes development

Notch2$^{+/-}$ was introgressed onto NOD mice and backcrossed for >10 generations. *Notch2*$^{+/-}$/NOD offspring were compared with WT littermates. A) Flow cytometry gating scheme of B220^{+}/IgM^{+} live lymphocytes for MZ markers (IgM^{hi}/IgD^{lo}/CD21^{hi}/CD23^{mid}) in WT (left) and *Notch2*$^{+/-}$/NOD (right) B cells. B-C) Average MZ B cell percentages (B), or total numbers of MZ B cells (C) in WT NOD (black bars) vs. *Notch2*$^{+/-}$/NOD (gray bars) mice. Error bars show SD for n = 6-8 age matched mice per group (12-16 weeks), from two experiments, **p < 0.001. D) Immunofluorescence staining of frozen spleen sections was

used to identify B cells (IgM^+, green) and metallophilic macrophages (MOMA-1^+, red). Representative 10X magnification images from n = 5 NOD mice (left) and n = 4 *Notch2*$^{+/-}$/NOD mice (right) are shown. Non-diabetic male and female mice were 14-16 weeks of age. White arrows indicate examples of MZ B cells located outside of the metallophilic macrophage ring that delineates the MZ. E) Female *Notch2*$^{+/-}$/NOD and WT NOD littermates were monitored for diabetes using weekly blood glucose levels. Kaplan-Meier survival curve shows percent non-diabetic (y-axis) vs. weeks of age for *Notch2*$^{+/-}$/NOD (gray line) vs. WT/NOD (black line). *Notch2*$^{+/-}$/NOD n = 10, WT NOD n = 7. No significant difference.

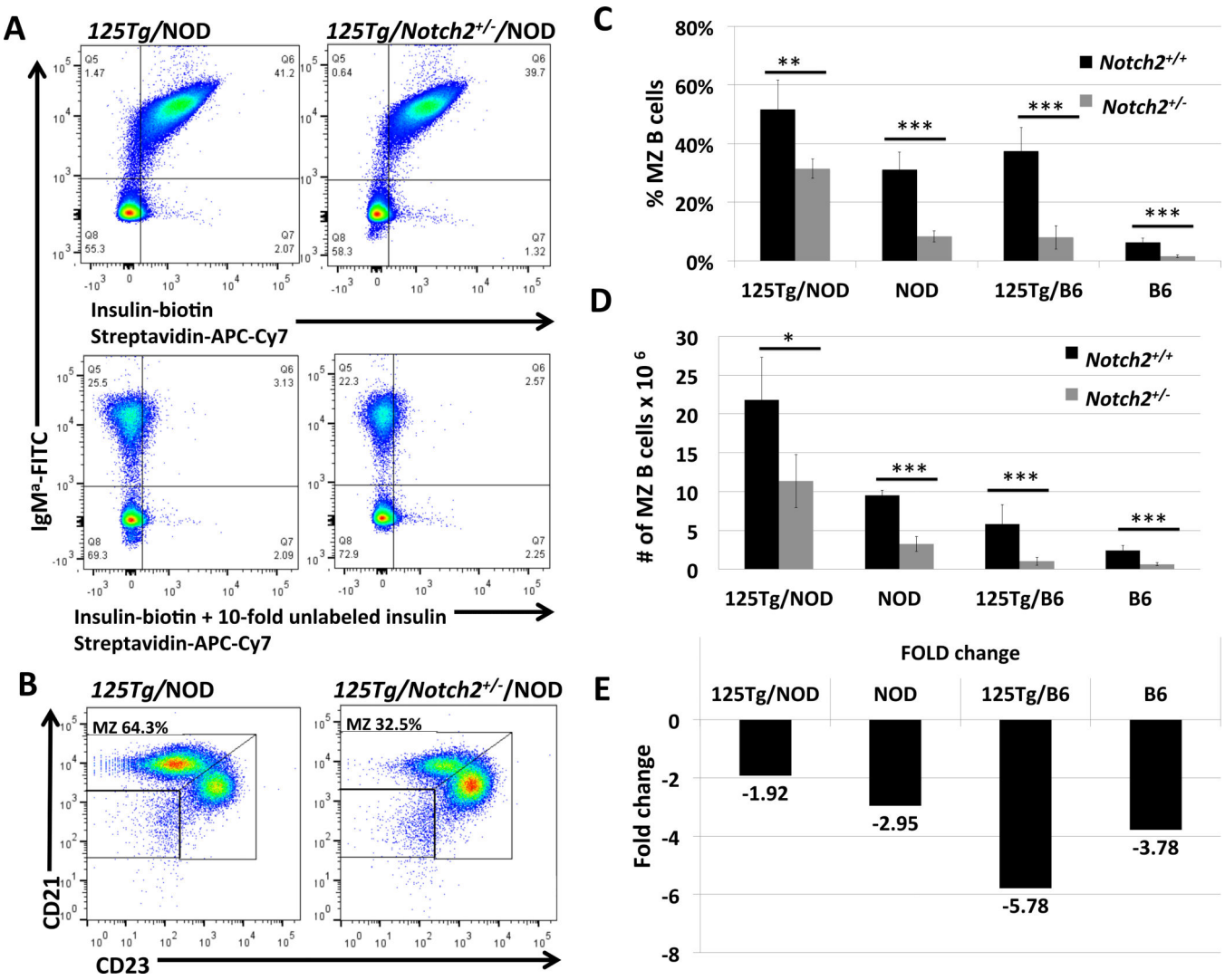

Figure 2. B cells with anti-insulin BCRs (125Tg) maintain an enlarged MZ in Notch2$^{+/-}$/NOD mice

Mice with B cells expressing transgenic anti-insulin BCRs (125Tg) were crossed with *Notch2*$^{+/-}$ mice on both NOD and C57BL/6 backgrounds, and MZ compartments were analyzed by flow cytometry. A) Flow cytometry showing biotinylated insulin-binding by transgenic IgM^{a+} B cells from 125Tg/NOD (upper left panel) and 125Tg/*Notch2*$^{+/-}$/NOD (upper right panel). Cells were gated on live lymphocytes. Lower panels show competitive inhibition, using ten-fold quantities of unlabeled insulin in parallel samples, to confirm insulin-specificity of binding in upper panels. B) Flow cytometry of live B220^{+}/IgM^{+} lymphocytes showing CD21/CD23 gating scheme used to identify MZ B cell populations for 125Tg B cells, which do not express IgD. C) Percent of B cells that are MZ B cells in *Notch2*$^{+/+}$ (black bars) vs. *Notch2*$^{+/-}$ (gray bars) for 125Tg and WT (endogenous BCRs) on both NOD and C57BL/6 backgrounds. D) Total numbers of MZ B cells for each genotype. E) Fold change in MZ numbers conferred by Notch2 haploinsufficiency (i.e., number of MZ in *Notch2*$^{+/+}$ divided by number of MZ in *Notch2*$^{+/-}$) for each genotype. For panels C-E, n = 3-5 mice per group for NOD strains, n = 6-10 mice per group for C57BL/6 strains, all

mice aged 12-13 weeks. * $p < 0.05$, ** $p < 0.01$, *** $p < 0.001$. Additional comparative significance values available in Supplemental Table I.

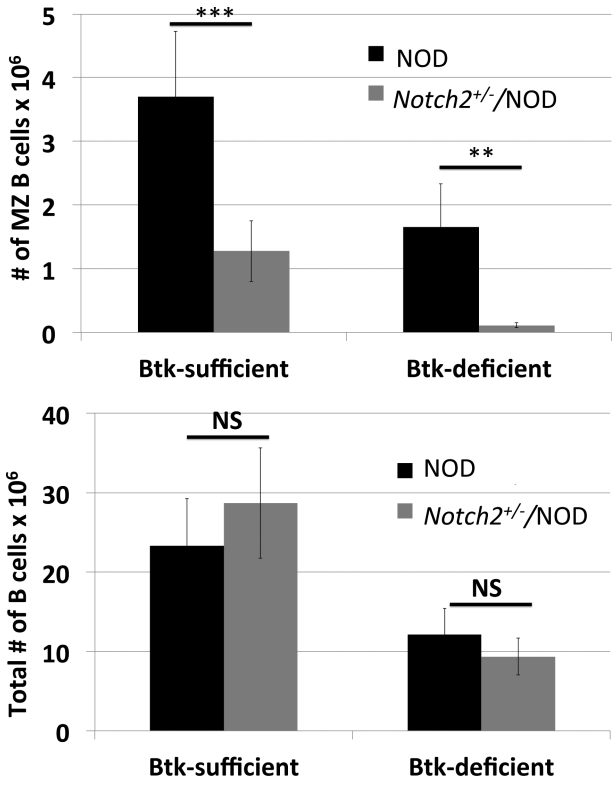

Figure 3. Notch2$^{+/-}$/NOD MZ compartment relies on Bruton's tyrosine kinase

Btk-deficient NOD mice were bred to *Notch2*$^{+/-}$/NOD mice and offspring were analyzed for MZ numbers by flow cytometry. Upper panel: MZ B cell numbers in NOD (black bars) and *Notch2*$^{+/-}$/NOD (gray bars), in the presence of BTK (*Btk*-sufficient, left) or absence of BTK (*Btk*-deficient, right). Lower panel: Total B cell numbers from the same animals. 12-13 week old mice, n = 6-8 per group. ** $p < 0.01$, *** $p < 0.001$, NS = no significant difference. Additional comparative significance values are available in Supplemental Table II.

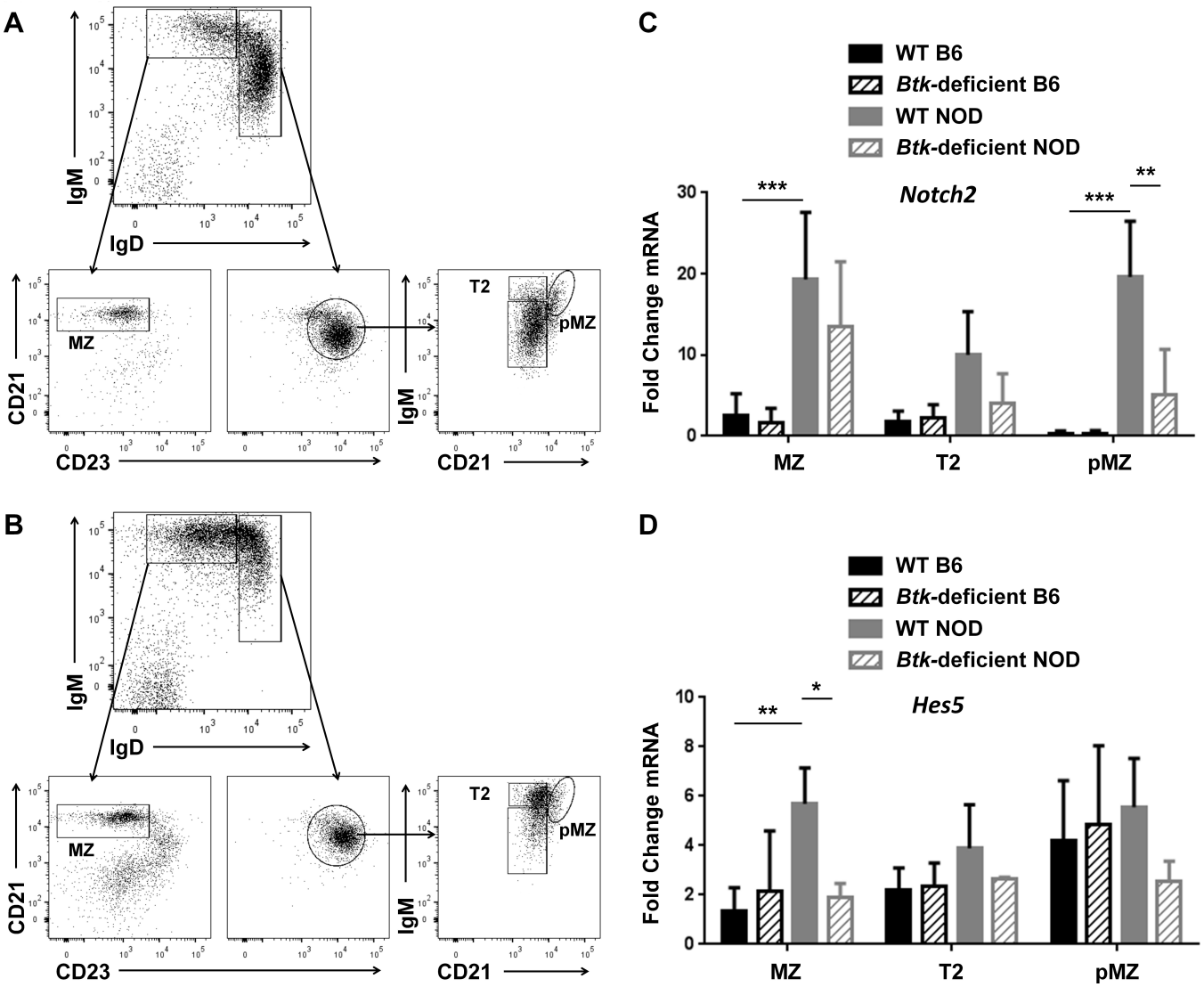

Figure 4. *Btk* deficiency negatively impacts expression of *Notch2* and its target *Hes5* in NOD, but not C57BL/6, B cells

$CD43^+$ cells were depleted using magnetic activated cell sorting and B cells from wild-type C57BL/6 (B6) or NOD, and Btk^{null} B6 or NOD were sorted into MZ, T2 and pMZ cell subsets using flow cytometry and analyzed by qRT-PCR for expression of *Notch2* and *Hes5* mRNA. A-B) Representative flow cytometry dotplots of wild-type (A) and Btk^{null} (B) NOD mice show the cell purification scheme; $IgM^{hi}IgD^{lo}$ B cells are gated by $CD21^{hi}CD23^{lo}$ for MZ cells, while $IgD^{hi}CD23^{hi}$ B cells are gated by $IgM^{hi}CD21^{lo}$ for T2 and $IgM^{hi}CD21^{hi}$ for pMZ. C-D) RNA was isolated from sorted B cells and analyzed by qRTPCR. Ct values of *Notch2* (C) and *Hes5* (D) were normalized to *HPRT* transcript levels and shown as fold change compared to the WT B6 MZ. Mean ± SD is shown for WT B6 (black, solid), Btk^{null} B6 (black, hatched), WT NOD (gray, solid) and Btk^{null} NOD (gray, hatched), n = 3-4 mice per genotype, * $p < 0.05$, ** $p < 0.01$ as calculated by two-way ANOVA with a Sidak correction for multiple comparisons.

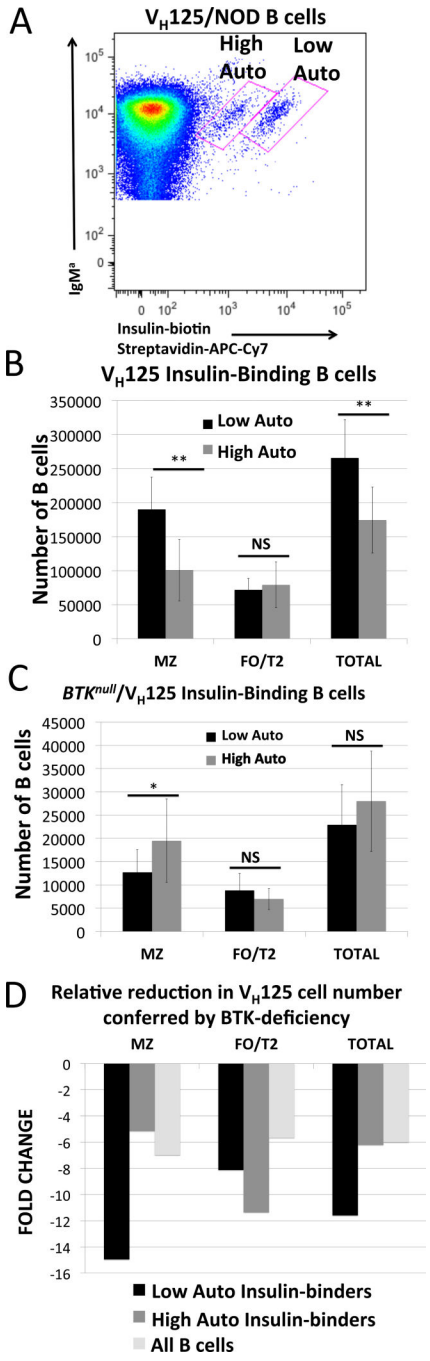

Figure 5. Differences in antigen-binding affect selection into the MZ and reliance on BTK

A) Flow cytometry analysis of insulin-binding populations in V_H125/NOD B cells freshly isolated from spleen. Two distinct insulin-binding populations are detected using biotinylated human insulin due to differences in BCR occupancy by endogenous rodent insulin *in vivo* (22). "High Auto" is used to designate the B cell population that binds rodent insulin better, corresponding with less binding by labeled human insulin as indicated by a lower MFI. The population for which labeled human insulin binds with increased intensity is designated "Low Auto." B) Number of cells from these two populations (Low Auto, black;

High Auto, grey) found in the MZ and FO of n = 8 V_H125/NOD mice. C) *BTK*^{null}/V_H125/NOD cell populations enumerated as in panel B, n = 12 mice. D) Fold change in cell numbers conferred by BTK-deficiency (i.e., number of cells in V_H125/NOD divided by number of cells in *BTK*^{null}/V_H125/NOD for each subset). Error bars represent standard deviation. * $p < 0.05$, ** $p < 0.01$, NS = no significant difference. Additional comparative significance values are available in Supplemental Table II.

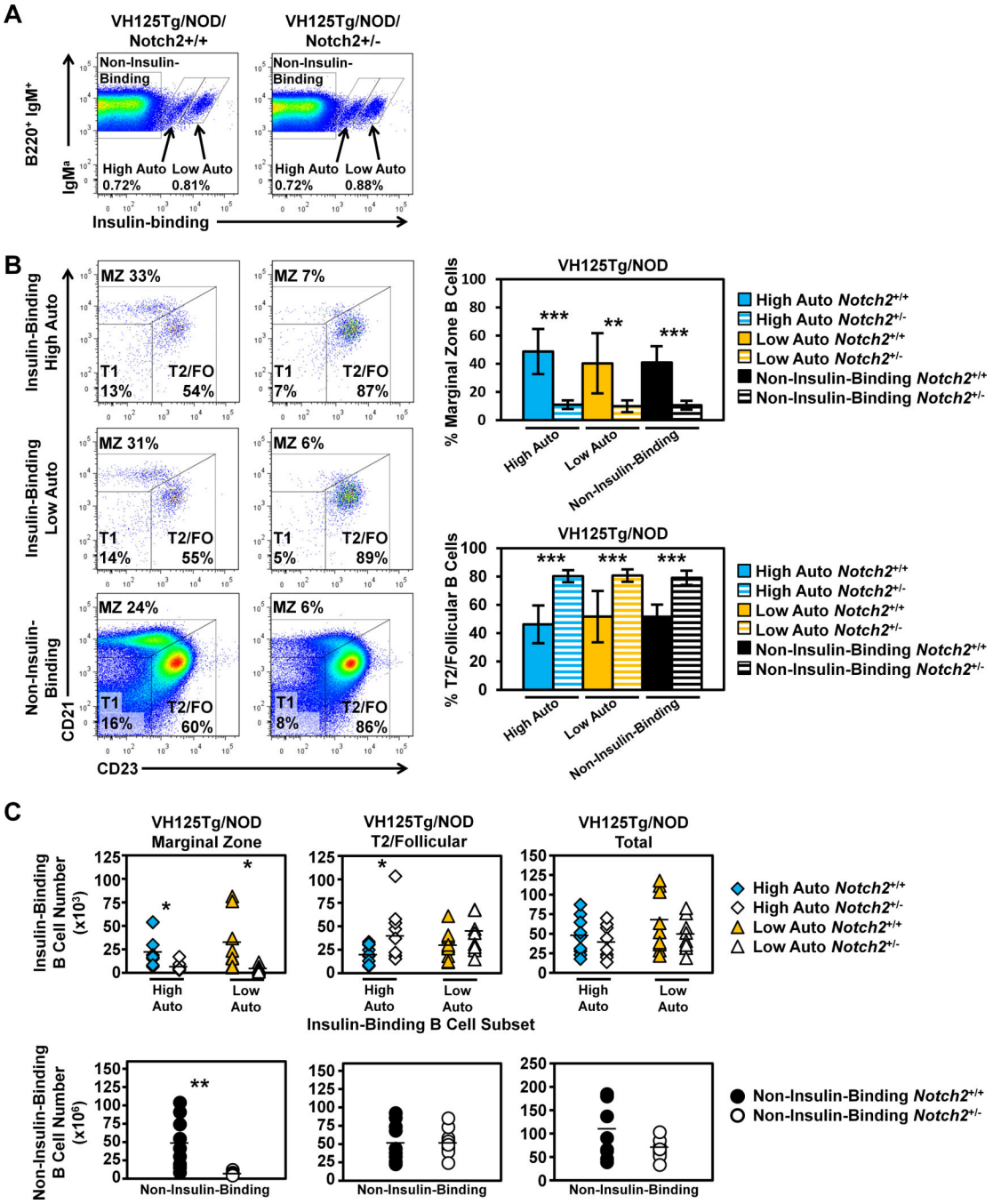

Figure 6. All V_H125Tg/NOD insulin-binding B cells rely on Notch2 for MZ selection, but not for survival

A) Flow cytometry analysis of B cells ($B220^+$ IgM^+ live lymphocytes) from V_H125Tg/NOD (left) vs. *Notch2*$^{+/-}$/V_H125Tg/NOD (right) mice. B) High Auto (top) or Low Auto (middle) insulin-binding B cells, or non-insulin-binding B cells (bottom) were further separated into MZ ($CD21^{high}$ $CD23^{mid}$) and T2/FO ($CD21^{mid}$ $CD23^{high}$) subsets. The average ± SD percentage of MZ or T2/FO insulin-binding High Auto (blue), insulin-binding Low Auto (orange), or non-insulin-binding (black) is shown to the right; *Notch2*$^{+/+}$ (solid), *Notch2*$^{+/-}$ (striped). C) The number of High Auto (blue diamonds) or Low Auto (orange triangles)

insulin-binding B cells found in the MZ (left), T2/FO (middle), or Total (right) B cell subsets is shown (top). The number of Non-Insulin-Binding (black circles) B cells found in the MZ (left), T2/FO (middle), or Total (right) B cell subsets is shown (bottom). Individual *Notch2*$^{+/+}$ (closed symbols) or *Notch2*$^{+/-}$ (open symbols) mice are plotted and the average is indicated. N = 8 V_H125Tg/NOD, n = 9 V_H125Tg/*Notch2*$^{+/-}$/NOD male and female 7-12 week old mice, * $p < 0.05$, ** $p < 0.01$, *** $p < 0.001$.

Table I

1
.

Idd Locus/ Chromosome	Linkage Marker
Idd1=H2g7/17	D17Mit34=C4
Idd3/3	D3Mit95
Idd4/11	D11Mit320
Idd5/1	D1Mit 18
Idd6/6	D6Mit339
Idd7/7	D7Mit20
Idd8, Idd12/14	D14Mit110
Idd8, Idd12/14	D14Mit222
Idd9,Idd11/4	D4Mit59
Idd10/3	D3mit103
Idd13/2	D2Mit395
Idd14/13	D13Mit 61
Idd15/5	D5Mit48

1 *Idd* loci genotyped to ensure NOD homozygosity in breeding pairs used for backcrossing at the 3rd through 10th generations.